Journal of Earth Science, Vol. 24, No. 6, p. 1044–1055, December 2013
Printed in China
DOI: 10.1007/s12583-013-0382-6 *ISSN 1674-487X*

Accelerated Thinning of Hei Valley No. 8 Glacier in the Tianshan Mountains, China

Zhen Wu*(武震), **Shiyin Liu** (刘时银), **Shiqiang Zhang** (张世强), **Donghui Shangguan** (上官冬辉)
State Key Laboratory of Cryospheric Science, Cold and Arid Regions Environmental and Engineering Research Institute, Chinese Academy of Sciences, Lanzhou 730000, *China*

ABSTRACT: Two field surveys on the thickness of Hei Valley No. 8 Glacier (H8) on the southern slope of Mount Bogda in the Tianshan (天山) Mountains using ground-penetration radar (GPR) were carried out in August 2008 and September 2009. Comparisons of the observed change in glacier thickness using GPR and ablation stakes suggest that GPR observations have high accuracy. Thus, the thickness change for H8 during 2008–2009 was estimated using GPR data. Digital elevation models obtained from topographic maps and the Shuttle Radar Topography Mission were used to analyze ice-elevation changes of H8 between 1 969 and 2 000 m a.s.l.. The results show that H8 has continually thinned, and the thinning rate has increased gradually. The thinning of ablation areas of H8 increased from 0.42±0.56 m/a in 1969–2000 to 1.47±0.79 m/a in 2000–2008, and then accelerated to 1.92±0.98 m/a in 2008–2009. The retreat of the glacier terminus has had a similar pattern. The distribution of the temperate-ice zone of H8 as determined from GPR data also implies that H8 has experienced strong melting from 2008 to 2009, which indicates that temperature rises have not only enhanced glacial surface melting and prolonged melting periods, but also changed the englacial structure and increased the water content of glacier, both of which probably lead to the acceleration of glacial thinning.
KEY WORDS: Hei Valley No. 8 Glacier (H8), ground-penetrating radar, ice-elevation change, thinning retreat, Tianshan.

INTRODUCTION

Glaciers are considered to be both a product and indicator of climatic change (Meier et al., 2007). Global warming since the Little Ice Age (LIA) has greatly reduced glacier coverage worldwide, and raised the equilibrium line altitudes of many glaciers (Aizen et al., 2007; Lioubimtseva and Cole, 2005; Liu et al., 2003; Su and Shi, 2002). The melting of polar and mountain glaciers is considered to be a main cause of the sea-level rise (Meier et al., 2007; Kaser et al., 2006; Braithwaite, 2002; Su and Shi, 2002), so it is important to understand the responses of glaciers to climate generally so as to be able to assess regional climate change (Annina et al., 2012; Liu et al., 2010; Christoph et al., 2007). Meanwhile, meltwater is regarded as an important water source in arid and semiarid regions, and plays a vital role in daily life, agricultural development, the raising of livestock and industrial development (Ding et al., 2006; Yao et al., 2004). To predict the future glacial response to climate,

This study was funded by the Project of the Knowledge Innovation of Chinese Academy of Sciences (No. KZCX2-YW-GJ04) and Postdoctoral Projects of China (Nos. 2012M 521817 and 2013M 5320 96).
*Corresponding author: wuzhen@lzb.ac.cn

Manuscript received April 23, 2013.
Manuscript accepted October 12, 2013.

it is necessary to understand the variation trends of the glacier length, area, retreat rate, thickness and other parameters in different periods (Meier et al., 2007; Oerlemans, 2005).

Remote sensing techniques have been applied to the Tianshan Mountains of Central Asia. Changes in the extent of 335 glaciers among the end of the LIA (mid-19th century), 1990 and 2003 have been estimated through the delineation of glacier outlines and LIA moraine positions in Landsat Thematic Mapper (TM) and Advanced Spaceborne Thermal Emission and Reflection Radiometer (ASTER) imagery for 1990 and 2003, respectively. By 2003, the glacier surface area had decreased by 19% from the LIA value, which constitutes a 76 km^2 reduction in the glacier surface area. The mapping of 109 glaciers using 1 : 25 000 maps for 1965 revealed that the glacier surface area decreased by 12.6% between 1965 and 2003 (Kutuzov and Shahgedanova, 2009). In addition, global positioning system (GPS) (Shangguan et al.,

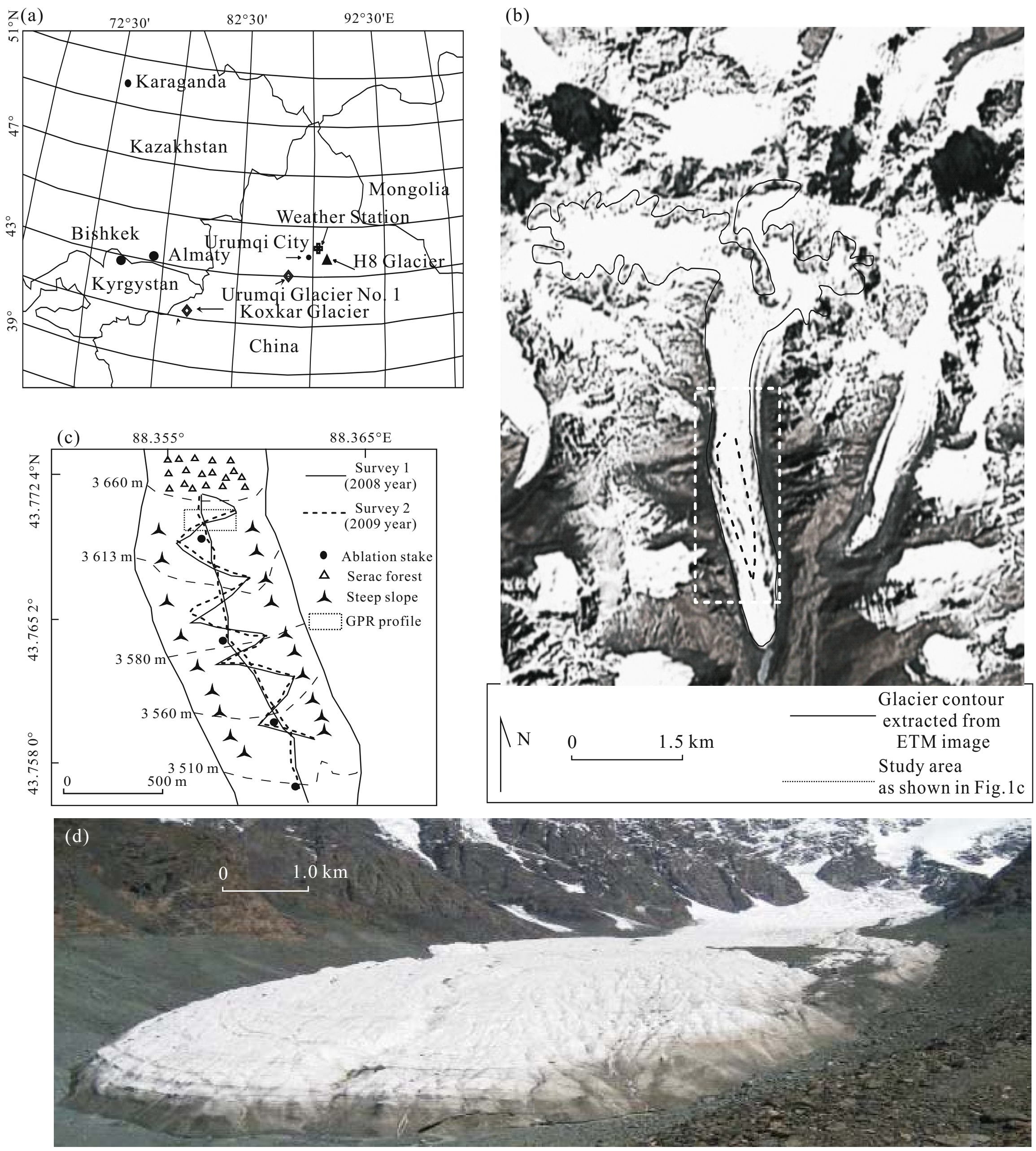

Figure 1. (a) Location of the No. 8 Glacier in the Hei Valley; (b) location of the No. 8 Glacier extracted from an Enhanced Thematic Mapper image; (c) schematic diagram of the track line of the GPR in August and September; (d) a picture of the termination of the glacier (taken on September 14th, 2009).

2010, 2009), ground-penetrating radar (GPR) (Jevrejeva et al., 2008; Bhosle et al., 2007; Al-Qadi and Lahouar, 2005), mass balance, and degree-day model (Zhang et al., 2010; Zhang et al., 2005; Bamber, 1987) studies have shown that there has been a significant effect of climate warming on glaciers in the Tianshan region in recent years.

In previous study, the mass balance has been regarded as the most important parameter in glacial variation and climate change (Vincent et al., 2002; Etzelmüller et al., 1993). In China, however, only Urumqi Glacier No. 1 has been subjected to systematic mass-balance measurements for nearly 50 years (Wang et al., 2011; Anderson et al., 2006; Braithwaite, 2002). Ice surface-elevation change is also an effective parameter for estimating the mass balance of a glacier for which there is a lack of observations through comparing a current digital elevation model (DEM) and an older DEM or topographic map (Shangguan et al., 2010, 2009). In addition, the mass loss can be extracted from thickness data for two periods (Andrea, 2009). In this study, we use GPR data for two periods to acquire the glacial mass loss, and compare with data recorded using ablation stakes to verify accuracy. The geological uses of GPR include the mapping of englacial structures and ice thickness (Bennett et al., 2009; Binder et al., 2009; Rippin et al., 2003; Gogineni et al., 2001; Moorman and Michel, 2000; Welch et al., 1998; Moore et al., 1989). The development of GPR technology has increased its accuracy, which in turn has allowed the determination of the change in thickness over a short time scale.

Not only does a glacier thin during the ablation season, but there is also meltwater infiltration through crevasses and moulins on the surface of the glacier. The englacial hydrological condition also changes. For instance, meltwater is channeled to temperate ice beneath the cold surface ice layer through surface crevasses and moulins (Murray et al., 2000; Moore et al., 1999; Macheret and Zhuavlev, 1993). A pure-ice body has a smooth representation in GPR, whereas the presence of water introduces noise. The comparison of ice-core data with radar image data has demonstrated that that GPR effectively distinguishes cold ice from temperate ice (Dowdeswell and Evans, 2004; Pettersson et al., 2003; Moore et al., 1999). Therefore, the extent of temperate ice can be regarded as a reference index of englacial ablation.

The thickness of Urumqi Glacier No. 1 and that of the Koxkar Glacier in the Tianshan Mountains have been investigated several times between 1970 to 2000, but comparison of the results is difficult because of the differences in survey locations and GPR instruments. In this study, we use the same Pulse Ekko-Pro GPR system to record data once in 2008 and once in 2009 on two measurement tracks that correspond to basically the same positions and have good comparability. Additionally, we use ablation stakes for the same period to verify the thickness data. This allows the accurate acquisition of the variation in ice thickness and englacial structure.

STUDY AREA AND METHOD

Site Description

The No. 8 Glacier in the Hei Valley (H8) (43°44'N–43°47'N, 88°19'E–88°22'E) (Fig. 1b) is located on the southern slope of Bogda Peak in the Tianshan Mountains. The glacier is regarded as a continental glacier (Hu and Li, 1989) and has a wide accumulation region with firn snow. H8 terminates at an altitude of 3 350 m a.s.l., has a high point at approximately 5 400 m a.s.l.. and has an area of 13.07 km^2. A field survey found that there are a great number of seracs above an altitude of 3 700 m a.s.l., there are irregularities of the glacial surface over most of the ablation area, and there are many supraglacial rivers and melting caves.

Equipment and Method

This study conducted two repeat investigations of H8 on August 3rd and 4th, 2008, and on September 14th and 15th, 2009, using the Pulse Ekko-Pro GPR manufactured by Sensors & Software Inc., Canada. The transmitting-receiving antennae were arranged in parallel at a distance of 4 m and transverse to the profile direction. The glacier's complex surface relief made working with GPR difficult and the handheld approach was the most effective method for surveying.

The GPR profiling was run in a common offset mode and traces were triggered artificially. Data were obtained over approximately 10 km between altitudes of 3 480 and 3 690 m a.s.l.. The profiles were recorded at one trace per meter, and each trace was resolved using 32-bit samples, which ensured the horizontal resolution of the section of measurement. Data for the two measurement tracks correspond to basically the same positions and have good comparability. Considering the different aiming depths and glacial locations, various time windows of 2 800–3 200 ns were adopted. A GPS device manufactured by Beijing UniStrong Science & Technology Co. Ltd. was used to position each profile. The standard error of the GPS device was 0.01 m±1 ppm (horizontal error) and 0.02 m±1 ppm (vertical error) under the conditions of the survey and signal reception. However, surveys of surfaces with geodetic-quality GPS receivers in real-time kinematic differential mode typically lead to horizontal and vertical survey errors (Rivera et al., 2005), which meets GPR data processing and analysis.

Radiowave velocities were calculated on the basis of the travel time to a point diffractor observed in the radar records. Only symmetric diffraction hyperbolae, which correspond either to point or horizontal linear diffractors crossed by the radar profile, were used. Features such as water-filled channels were detected and measured using multiple profiles to estimate the radiowave velocity correctly. This study adopted a radar wave velocity of 0.167 m/ns.

Error in GPR Measurement

There are two main aspects to GPR measurement error: the antenna distance and antenna resolution. In terms of antenna distance, the transmitter and receiver antennas are placed parallel. The glacier's complex undulating surface terrain affects the antenna distance in the measurement. Assuming the greatest change in antenna distance is 2 m, there is ±0.2 m error per 100 m ice thickness. Since the maximum ice thickness obtained from GPR in this study is 250 m, the maximum error is ±0.5 m. In terms of antenna resolution, we use a 50 MHz bistatic antenna. There is a ±0.6 m error in identifying the bedrock interface. The total error is thus

$$EP_{\text{error}} = \frac{H}{100} \times 0.2 + 0.6$$

Topographic, SRTM DEM and TM Image

The data used in this study include 1 : 50 000 topographic Chinese Military Geodetic Service maps for 1969. The vertical error in glacier extent is ±19 m for slopes less than 15° and ±11 m for slopes greater than 15° (Kaab, 2005). We extracted topographic contour data to interpolate to get the 1969 DEM data, and represent values that have been orthorectified to the Universal Transverse Mercator (UTM) coordinate system and referenced to the World Geodetic System 1984 (WGS84).

Radar topology mapping data recorded by the Shuttle Radar Topography Mission (SRTM) (http://srtm.csi.cgiar.org/index.asp) in 2000 (National Imagery and Mapping Agency in cooperation with the National Aeronautics and Space Agency (NASA)) were also used (Table 1). We selected 80 random points in surrounding non-glacierized areas at elevations below 4 400 m a.s.l. and with slope less than 15°, and compared the DEMs. The results revealed a mean difference of 6.24 m. However, we did not calculate systematic errors because we lacked sufficient information to quantify their magnitudes. Instead, we used the maximum errors for the SRTM data in 2000. We also acquired Aerialphotographs (1970), Landsat Multispectral Scanner TM (1997), and Enhanced Thematic Mapper (2010, 2007) images (dataset provided by the International Scientific Data Service Platform, Computer Network Information Center, Chinese Academy of Sciences (http://datamirror.csdb.cn)). Error estimation for TM is quantified based on the image spatial resolution or map scale (1 : 100 000 and 1 : 50 000) are equated respectively to spatial resolutions of 30 and 15 m in pixel size). To calculate changes between two images, an average spatial resolution of these two maps is assumed for error determination.

RESULTS

Comparison of Ablation Stake and GPR

Because GPR data can reflect the thickness change on survey regions, we extracted ablation-stake data for the same period to compare with GPR data (Fig. 2c) and provide a reference for GPR data accuracy. It should be noted, due to the location of ablation

Table 1 Topographic maps and satellite remote-sensing data

Data	Satellite sensor/map	Source	Spatial resolution/ map scale
Sep. 1966	Topographic map	Chinese military geodetic service	1 : 50 000
Dec. 2000	SRTM3 DEM	USGS/NASA	30 m
Aug. 1970	Aerialphotographs	USGS/NASA	28.5 m
Sep. 1997	Landsat TM	USGS/NASA	28.5 m
Oct. 2007	Landsat TM	USGS/NASA	15 m
Aug. 2010	Landsat TM	USGS/NASA	15 m

stake may move along with ice flow processes, in this study, we compared the glacier thickness change monitored by GPR survey with that observed by ablation stakes at the same positions as these stakes located in 2009. The ablation results were 1.5±0.96 m and 3.32 m for the GPR and ablation stake except at the position with altitude of 3 629 m a.s.l., where there had been large ablation. At altitudes of 3 504, 3 549 and 3 596 m a.s.l., GPR measurements were 2.87±0.91, 1.91±0.87, 1.65±0.84 m and ablation stake measurements were 3.35, 1.36 and 1.53 m, respectively, showing good agreement (the magnitudes of melting recorded with ablation stakes are all within the range of GPR errors). To analyze the sources of error, we extracted the supraglacial slope at four locations. The supraglacial slope is only greater at the position with altitude of 3 629 m a.s.l. in Fig. 2, which suggests that the local terrain is likely to dominate the characteristics of the ice surface ablation; e.g., there is

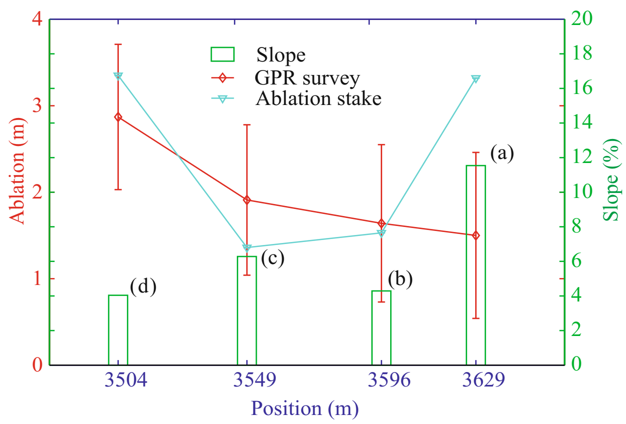

Figure 2. Comparison of the GPR survey (including errors) and ablation stake survey, and the slope at difference positions.

fast supraglacial flow for steep slopes, and the slope affects the amount of solar radiation received. In this paper, we consider that measurements made with an ablation stake contain large errors for steep slopes, and GPR data are relatively accurate.

Thickness Changes from 2008 to 2009

As the location surveyed did not extend to the glacial boundary, interpolation borders cannot be set to zero. Only a limited part of the ablation area of the glacier was analyzed for ice-elevation change so we only interpolate ice thickness in the surveyed area. Ice-thickness distribution maps (Figs. 3a and 3b) were obtained by interpolating the GPR thickness data obtained in 2008 and 2009 employing ordinary kriging. From comparison of the two survey results (Fig. 3c), it is seen that the ice thickness in the measurement region decreased between 1 and 3 m, with annual thinning of 1.92±0.98 m. It is seen from the spatial distribution of the ice thickness that the higher the altitude, the less the decrease in ice thickness. For instance, the ice thickness decreased less than 1.5 m above an altitude of 3 600 m a.s.l. but decreased 2 m below that altitude.

Thickness Change from 1969 to 2009

Due to the difference of resolution between 1969 topographic map, 2000 DEM and GPR, we interpolate the topographic map and DEM to make them get a uniform 10 m resolution with GPR data. Table 2 presents the annual change in elevation for H8 from 1969 to 2009. The table reveals that H8 has been thinning since 1969, the average annual thinning in the

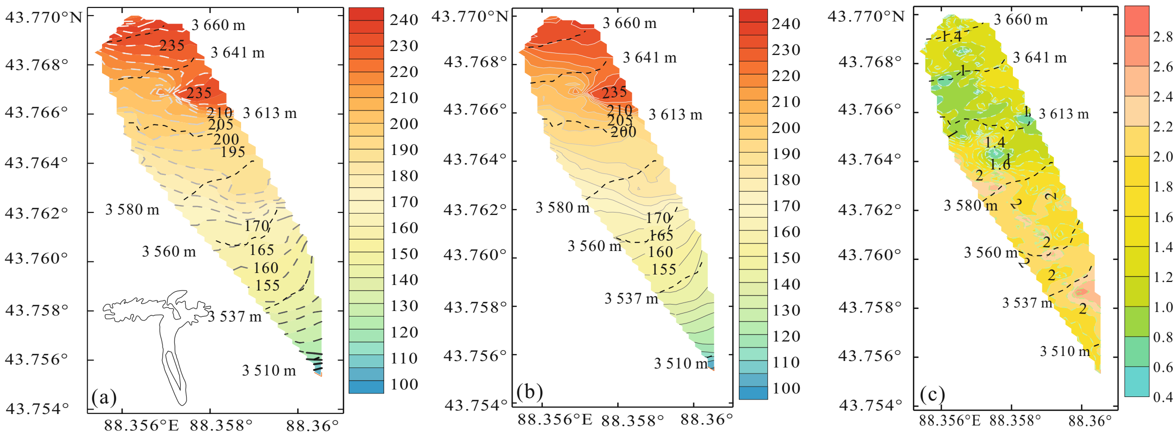

Figure 3. Map of the calculated ice thickness in 2008 (a) and 2009 (b); (c) showing the difference in ice thickness between a and b.

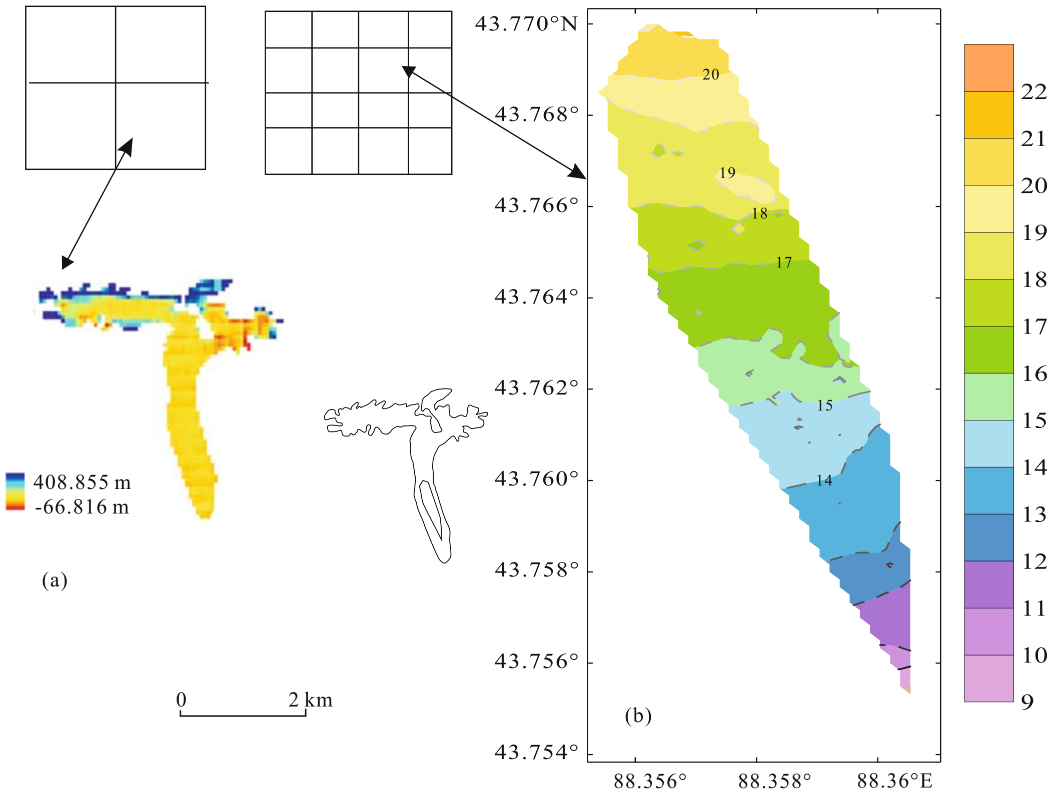

Figure 4. (a) Map of the difference in elevation at entire glacier area between topographic maps for 1969 and 2000 SRTM data; The interpolated DEM at GPR survey location extracted from map (a), which have a uniform 10 m resolution with GPR data (b).

surveyed area was 0.42±0.56 m/a from 1969 to 2000 (Fig. 4), 1.47±0.79 m/a from 2000 to 2008 and 1.92±0.98 m/a from 2008 to 2009, the annual change of thickness from 2008 to 2009 was 4.6 times that of 1969–2000 and 1.3 times that in 2000–2008, and this change in elevation accelerated remarkably after 2000.

Variation in the Distribution of Ice Temperate

Figure 5 presents a dense chaotic return zone. Generally, when electromagnetic waves meet materials with particle size less than the radar resolution, the electromagnetic wave is not reflected. According to the theory of Kotlyakov and Plewes, (1) water is known to cause such perturbations in the wave profile (Kotlyakov and Macheret, 1987); (2) during an

Table 2 Thickness changes during different periods (change in elevation ($m \cdot a^{-1}$))

Time period	The position of ablation stake (m a.s.l.)			
	3 504	3 549	3 596	3 629
1969–2000	0.58±0.55	0.54±0.55	0.45±0.55	0.32±0.55
2000–2008	1.84±0.796	1.31±0.786	1.49±0.792	1.16±0.785
2008–2009	2.87±0.91	1.91±0.87	1.65±0.84	1.5±0.96

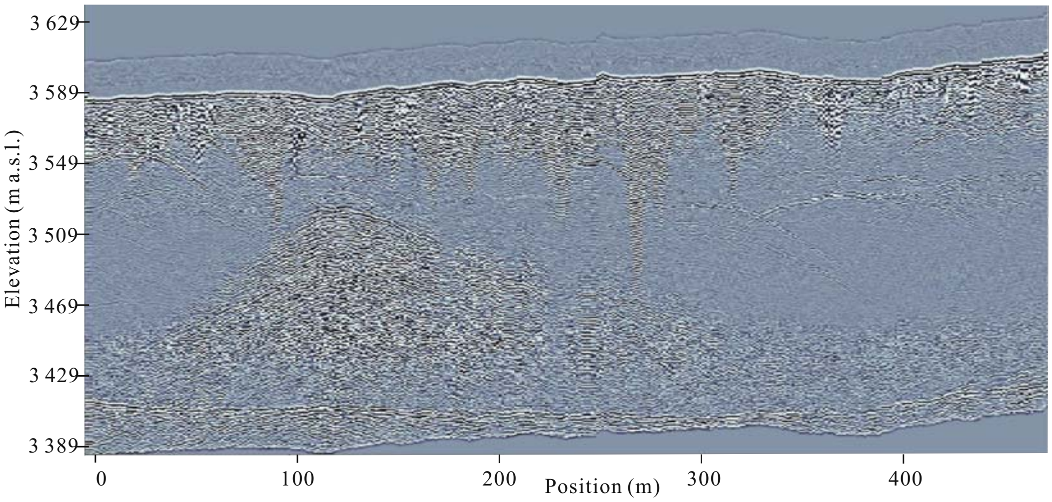

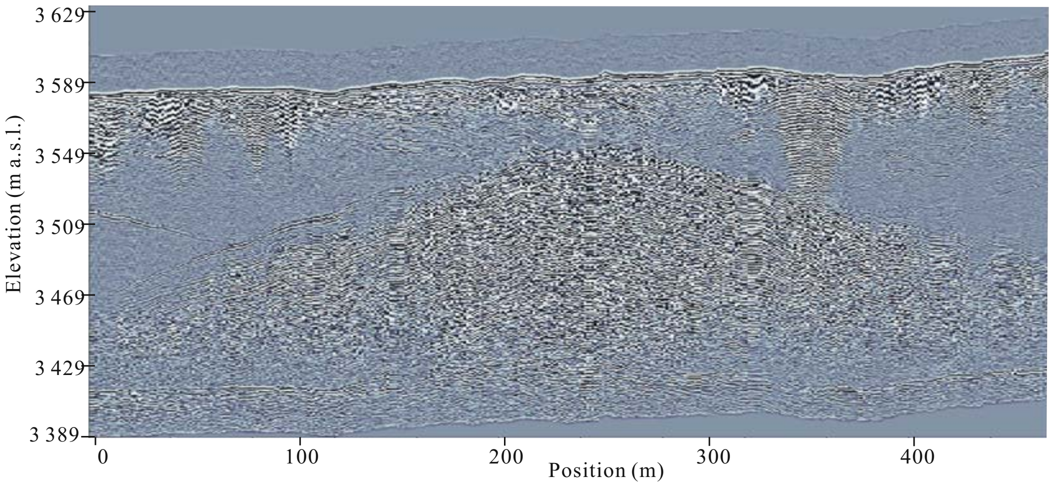

Figure 5. Comparison between 2008 (a) and 2009 (b) indicating a change in the temperate-ice thickness; the location of the section is position 1 in Fig. 1c.

ablation season, electromagnetic pulses can be scattered owing to enhanced melting and/or refreezing leading to englacial heterogeneities (Irvine-Fynn et al., 2006; Plewes and Hubbard., 2001). It is concluded that the dense chaotic return zone is a product of an ice body containing water, which is similar to the findings of Irvine-Fynn et al. (2006), Pettersson et al. (2003), and Björnsson et al. (1996). Because the surface melt water usually have a positive temperature and vary between 0.1 and 4.0 ℃ in the rapid ablation period, with the increasing of supraglacial melt water, meltwater will transfers more heat to englacial ice-body. Moore et al. (1999) even estimate the temperate ice to have 1%–2% water content. Maximum concentrations of approximately 4% water content were associated with ice beneath surface crevassing and moulins that allow water to be channeled to the temperate-ice aquifer beneath the surface cold ice layer (Moore et al., 1999), which shows change in spatial distribution of temperate ice can reflect the glacial ablation condition. Maps of the approximate two-dimensional spatial distribution of temperate ice were constructed for each GPR survey (Fig. 6). The extent of the temperate-ice distribution in September 2009 was greater than that in August 2008, and the region uplifted by temperate ice was mainly at high-altitude locations in the surveyed area, that is probably because the ablation of supraglacial ice-body in high-altitude position have intensified for climate warming, which lead that more melt water permeate into ice-body through crevasses or moulins, increasing englacial water content at the same high-altitude position, which indicates that the ice body in high-altitude position of surveyed area is in a phase of increasing ablation.

CLIMATE CHANGES AND GLACIER CHANGE

The average air temperatures in September and October from 1952 to 2007 recorded at the Urumqi Weather Station near H8 have rapidly increased, at rates of 0.09°/10 years and 0.34°/10 years, respectively, whereas the average temperature in August has decreased slightly at a rate of 0.015°/10 years (Fig. 7), indicating that the glacial ablation period for H8 may have been prolonged in the context of climate warming.

The altitude of the terminus was 3 373, 3 380, 3 385, 3 401 and 3 409 m a.s.l. in 1970, 1989, 1997, 2007 and 2010, respectively (Table 3). The annual rate of retreat of the terminus was 0.36, 0.625, 1.6, and 2.66 m/a between these years. Comparison of the terminal positions reveals that the rate of terminal retreat has had a tendency to increase. Particularly, during 1997–2007 and 2007–2010, the rate of terminal retreat compared with the rate for the previous period increased by 1 $m \cdot a^{-1}$, which indicates that the amount of H8 glacial meltwater is increasing.

Research in the 1980s on H8 found that the end of the ablation period was September 19 and the amount of glacial drainage decreased after this day (Hu et al., 1990; Hu and Li, 1989). The GPR survey results show that the range of the temperate-ice distribution in September 2009 was greater than that in August 2008, indicating that there was much meltwater intermingling with the ice body through crevasses and moulins. At the same time, the greater abundance of englacial cavities and the development of channels offer much more reserve space for glacial meltwater, and complex englacial conflux paths increasing the conflux time may also result in meltwater diffusing in the ice body and accelerating englacial ablation (Irvine-Fynn et al., 2006). The areal distribution of the temperate ice zone of H8 Glacier, and change in its radar characteristics over time indicated variable water content in response to an evolving hydrological drainage system within the glacier. The increase in water stored within the temperate zone has potentially significant connotations, in particular relating

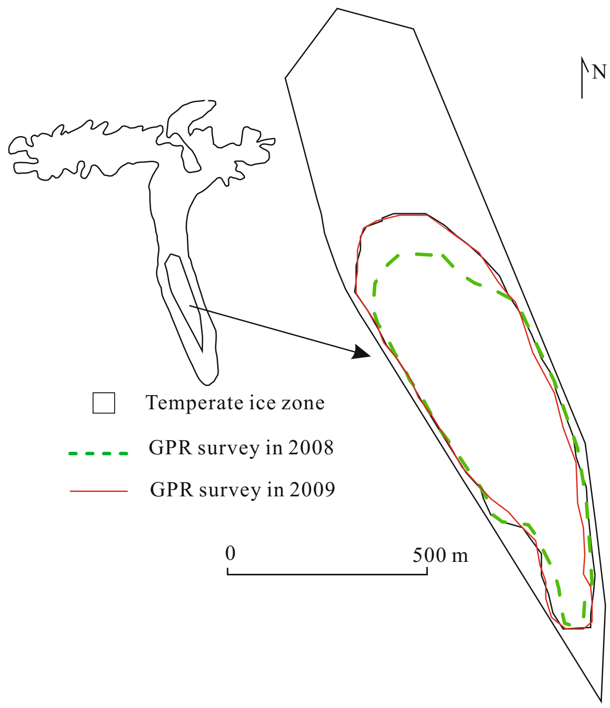

Figure 6. Variation in the temperate-ice distribution between 2008 and 2009.

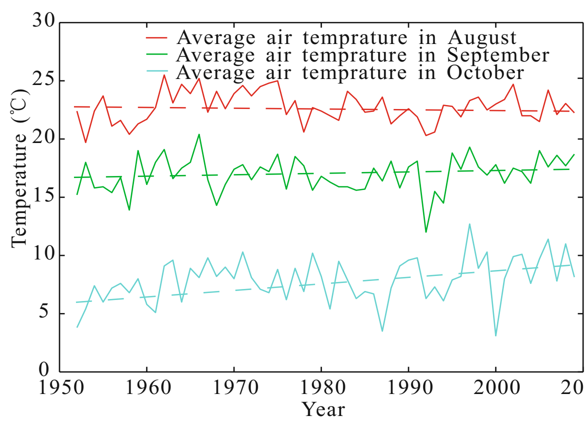

Figure 7. Comparison of air temperature data and the tendencies in August, September and October from 1952 to 2007 as recorded at the Urumqi Weather Station near H8 Glacier.

Table 3 Variation in the terminal position of H8 since 1970

Time	Altitude of terminus (m a.s.l.)	Source	Period	Annual Variation of terminus position (m/a)
1970	3 373	TM image	1970–1989	0.360±1.70
1989	3 380	Wang (1991)	1989–1997	0.625±2.40
1997	3 385	TM image	1997–2007	1.600±1.30
2007	3 401	TM image	2007–2010	2.660±3.75
2010	3 409	TM image		

to the hydrological dynamics and water released from high latitude glaciers subject to retreat and projected climatic change.

Comparisons are made with other glaciers in the Tianshan Mountains in Table 4. The thinning of H8 is greater than that of the Koxkar Glacier and Urumqi Glacier No. 1. Besides the above mentioned regional climate warming, glacier change also is subject to some non-climate factors, as for the difference of ablation in adjacent glaciers, the thinning of H8 is greater than Urumqi Glacier No. 1, for instance, flat ice surface keep melt-water putaside, and steep terrain make melt-water drain, at the same time, difference slope will also affect the ice surface solar radiation, which shows glacial topographic factors can effect surface ablation and dynamic characteristics.

The distribution patterns and area of a glacier is a key factor influencing the glacier response to climate change (Genthon et al., 2009; Cannone et al., 2008), such as the larger the glacier area, the slower the absorbed heat can be transferred into the ice center (Wang et al., 2010; Li et al., 2007). H8 Glacier is longer, has a lingering tongue, and neither side of the ice body is close to bilateral bedrock, which would transfer much solar energy to the ice body. And a clean surface can absorb little sunlight on its surface due to its high albedo (Wang et al., 2011).

Furthermore, the thickness of debris-cover also has a difference effects among glacier ablation. Observations of ice ablation under a debris layer suggest that a very thin debris cover may accelerate melting, but when surface debris thickness is more than 3 cm it acts as an insulator against external temperature variations on the ice body (Han et al., 2010; Xie et al., 2007; Goodsell et al., 2005) there are very thin debris layers distributed on local location of H8 glacial surface, and this kind of status of debris cover may accelerate melting.

CONCLUSION

Through GPR investigation, we can conclude as following.

(1) The ice thickness in the measurement region of H8 decreased between 1 and 3 m, with annual thinning of 1.92±0.98 m, from 2008 to 2009. The annual change of thickness from 2008 to 2009 was 4.6 times that of 1969–2000 and 1.3 times that in 2000–2008. This change in elevation accelerated remarkably after 2000. We recorded GPR data twice, obtaining ice volumes in the surveyed area of 67.53×10^{-3} km^3 in 2008 and 66.84×10^{-3} km^3 in 2009. From 2008 to 2009, the change in ice volume in the surveyed area was 0.000 69±0.000 395 3 km^3 or 1.02%±0.58%.

(2) The range of the temperate-ice distribution in

Table 4 Comparison of changes for typical monitored glaciers in western China in recent years

Glacier	Period	Annual change (m)	Source
H8 Glacier	2008–2009	1.92±0.98 (surveyed area)	This study
	1969–2009	1.13±0.30 (surveyed area)	This study
Koxkar Glacier	2000–2009	1.50±0.73 (surveyed area)	This study
Urumqi Glacier	1981–2006	1.00±0.50(ice tongue)	Xie et al., 2006
No.1	1981–2006	0.56±0.16 (main streamline in east branch）	Li et al., 2007

high-altitude in the surveyed area, indicating that the ice body in the surveyed area is in a phase of increasing ablation.

(3) Comparison of TM images for different years showed that there was greater change in the altitude of the terminus around 2009, indicating an escalating rate of glacial retreat.

(4) Comparison of changes of H8 with other glaciers by field measurement over eastern Tianshan indicated that the ablation area is most serious for glaciers in the middle of eastern Tianshan, followed by the west, and then the east. The climatic sensitivity of these glaciers not only depends on regional climate variability but also on local topographic effects.

ACKNOWLEDGMENTS

We express our thanks to Gang Li, Zhaojin Dong, Yinsong Zhang for guidance and helpful during the field survey.

REFERENCES CITED

Aizen, V. B., Kuzmichenok, V. A., Surazakov, A. B., et al., 2007. Glacier Changes in the Tien Shan as Determined from Topographic and Remotely Sensed Data. *Global and Planetary Change*, 56(3–4): 328–340

Al-Qadi, I. L., Lahouar, S., 2005. Measuring Layer Thicknesses with GPR-Theory to Practice. *Construction and Building Materials*, 19(10): 763–772

Anderson, B., Lawson, W., Owens, L., et al., 2006. Past and Future Mass Balance of Ka Roimata o Hine Hukatere Franz Josef Glacier, New Zealand. *Journal of Glaciology*, 52(179): 597–607

Andrea, F., 2009. Calculation of Glacier Volume from Sparse Ice-Thickness Data, Applied to Schaufelferner, Austria. *Journal of Glaciology*, 55(191): 453–460

Annina, S., Tobias, B., Markus, S., et al., 2012. Climate Change Impacts on Glaciers and Runoff in Tien Shan (Central Asia). *Nature Climate Change*, 2(10): 725–731, doi:10.1038/nclimate1592

Bamber, J. L., 1987. Internal Reflecting Horizons in Spitsbergen Glaciers. *Annals of Glaciology*, 9: 5–10

Bennett, M. R., Cassidy, N. J. Pile, J., 2009. Internal Structure of a Barrier Beach as Revealed by Ground Penetrating Radar (GPR): Chesil Beach, UK. *Geomorphology*, 104(3–4): 218–229

Bhosle, B., Parkash, B. Awasthi, A. K., et al., 2007. Remote Sensing-GIS and GPR Studies of Two Active Faults, Western Gangetic Plains, India. *Journal of Applied Geophysics*, 61(2): 155–164

Binder, D., Bruckl, E., Roch, K. H., et al., 2009. Determination of Total Ice Volume and Ice-Thickness Distribution of Two Glaciers in the Hohe Tauern Region, Eastern Alps, from GPR Data. *Annals of Glaciology*, 50(51): 71–79

Björnsson, H., Gjessing, Y., Hamran, S. E., et al., 1996. The Thermal Regime of Sub-Polar Glaciers Mapped by Multi-Frequency Radio-Echo Sounding. *Journal of Glaciology*, 42(140): 23–32

Braithwaite, R. J., 2002. Glacier Mass Balance: The First 50 Years of International Monitoring. *Progress in Physical Geography*, 26(1): 76–95

Brandt, O., Langley, K., Kohler, J., et al., 2007. Detection of Buried Ice and Sediment Layers in Permafrost Using Multi-Frequency Ground Penetrating Radar: a Caseexamination on Svalbard. *Remote Sensing of Environment*, 111(2–3): 212–227, doi: 10.1016/ j.rse. 2007. 03. 025

Cannone, N., Diolaiuti, G., Guglielmin, M., et al., 2008. Accelerating Climate Change Impacts on Alpine Glacier Forefield Ecosystems in the European Alps. *Ecological Applications*, 18(3): 637–648

Christoph, S., Michael, S., César, A., et al., 2007. Glacier Inventory of the Gran Campo Nevado Ice Cap in the Southern Andes and Glacier Changes Observed during Recent Decades. *Global and Planetary Change*, 59(1–4): 87–100

Clarke, G., Goodman, R., 1975. Radio Echo Soundings and Ice-Temperature Measurements in a Surge-Type Glacier. *Journal of Glaciology*, 14(70): 71–78

Clark, D. H., Clark, M. M. Gillespie, A., 1994. Debris-Covered Glaciers in the Sierra Nevada, California, and Their Implications for Snowline Reconstructions. *Quaternary Research*, 41(2): 139–153

Ding, Y. J., Liu, S. Y., Li, J., et al., 2006. The Retreat of Glaciers in Response to Recent Climate Warming in Western China. *Ann. Glaciol*., 43(1): 97–105

Dowdeswell, J. A., Evans, S., 2004. Investigations of the Form and Flow of Ice Sheets Using Radio Echo-Sounding. *Rep. Prog. Phys*., 67(10): 1821–1861

Etzelmüller, B., Vatne, G., Degard, R. S., 1993. Mass Balance Changes of Surface Slope, Crevasse and Flow Pattern of Erikbreen, Northern Spitsbergen: An Application of a Geographical Information System. *Polar Research*, 12(2): 131–146

Gogineni, S., Tammana, D., Braaten, D., et al., 2001. Coherent

Radar Ice Thickness Measurements over the Greenland Ice Sheet. *Journal of Geophysical Research D*: *Atmospheres*, 106(24): 33761–33772

Genthon, C., Krinner, G., Castebrunet, H., et al., 2009. Antarctic Precipitation and Climate-Change Predictions: Horizontal Resolution and Margin Vs Plateau Issues. *Annals of Glaciology*, 50(50): 55–60

Goodsell, B. M., Hambrey, M. J., Glasser, N. F., et al., 2005. Debris Transport in a Temperate Valley Glacier: Haut Glacier D'Arolla, Valais, Switzerland. *Journal of Glaciology*, 51(172): 139–146

Han, H., Liu, S., Wang, J., et al., 2010. Glacial Runoff Characteristics of the Koxkar Glacier, Tuomuer-Khan Tengri Mountain Ranges, China. *Environmental Earth Sciences*, 61(4): 665–674

Hu, X. G., Li, N. J., 1989. A Stochastic Meltwater Runoff Model of Heigou Glacier No. 8 in the Southern Slope of Mt. Bogda. *Journal of Glaciology and Geocryology*, 11(3): 91–98 (in Chinese with English Abstract)

Hu, X. G., Li, N. J., Deng, S. M., 1990. Glacier Meltwater Runoff on the South Slope of the Bogeda Mt—Taking the Heigou as an Example. *Journal of Glaciology and Geocryology*, 12(1): 71–82 (in Chinese with English Abstract)

Irvine-Fynn, T. D. L., Moorman, B. J., Williams, J. L. M., et al., 2006. Seasonal Changes in Ground Penetrating Radar Signature Observed at a Polythermal Glacier, Bylot Island, Canada. *Earth Surface Process and Landforms*, 31(7): 892–909

Jevrejeva, S., Moore, J. C., Grinsted, A., 2008. Relative Importance of Mass and Volume Changes to Global Sea Level Rise. *J. Geophys. Res.*, 113(D8), doi:D0810 5.10.1029/2007JD009208

Kaab, A., 2005. Combination of SRTM3 and Repeat ASTER Data for Deriving Alpine Glacier Flow Velocities in the Bhutan Himalaya. *Remote Sensing of Environment*, 94(4): 463–474

Kaser, G. J., Cogley, M. B., Dyurgerov, M. F., et al., 2006. Mass Balance of Glaciers and Ice Caps: Consensus Estimates for 1961–2004. *Geophys. Res. Lett.*, 33(19): L19501 doi:10.1029/2006GL027511

Kotlyakov, V. M., Macheret, Y. Y., 1987. Radio Echo-Sounding of Sub-Polar Glaciers in Svalbard: Some Problems and Results of Soviet Studies. *Journal of Glaciology*, 9: 151–159

Kutuzov, S., Shahgedanova. M., 2009. Glacier Retreat and Climatic Variability in the Eastern Terskey-Alatoo, Inner Tien Shan between the Middle of the 19th Century and Beginning of the 21st Century. *Global and Planetary Change*, 69(1): 59–70

Li, Z. Q., Shen, Y. P., Wang, F. T., et al., 2007. Response of Glacier Melting to Climate Change—Take Urumqi Glacier No. 1 as an Example. *Journal of Glaciology and Geocryology*, 29(3): 333–342 (in Chinese with English Abstract)

Lioubimtseva, E., Cole, R., 2005. Impacts of Climate and Land-Cover Changes in Arid Lands of Central Asia. *Journal of Arid Environments*, 62(2): 285–308

Liu, Q., Liu, S. Y., Zhang, Y., et al., 2010. Recent Shrinkage and Hydrological Response of Hailuogou Glacier, a Monsoon Temperate Glacier on the East Slope of Mount Gongga, China. *Journal of Glaciology*, 56(196): 215–224

Liu, S. Y., Sun, W. X., Shen, Y., et a1., 2003. Glacier Changes since the Little Ice Age Maximum in the Western Qilian Mountains, Northwest China. *Journal of Glaciology*, 49(164): 117–124

Macheret, Y. Y., Zhuravlev, A. B., 1993. Velocity of Radio Waves in Glaciers as an Indicator of Their Hydrothermal State, Structure and Regime. *Journal of Glaciology*, 39(132): 373–384

Meier, M. K., Dyurgerov, U. K., Rick, S., et al., 2007. Glaciers Dominate Eustatic Sea-Level Rise in the 21st Century. *Science*, 317(5481): 1064–1067

Moore, J. C., Mulvaney, R., Paren, J. G., 1989. Dielectric Stratigraphy of Ice: A New Technique for Determining Total Ionic Concentrations in Polar Ice Cores. *Geophys. Res. Lett.*, 16(10): 1177–1180

Moore, J. C., Palli, A., Ludwig, F., et al., 1999. High-Resolution Hydrothermal Structure of Hansbreen, Spitsbergen, Mapped by Ground-Penetrating Radar. *Journal of Glaciology*, 45(151): 524–532

Moorman, B. J., Michel, F. A., 2000. Glacial Hydrological System Characterization Using Ground Penetrating Radar. *Hydrological Processes*, 14(15): 2645–2667

Murray, T., Stuart, G. W., Fry, M., et al., 2000. Englacial Water Distribution in a Temperate Glacier from Surface and Borehole Radar Velocity Analysis. *Journal of Glaciology*, 46(154): 389–398

Oerlemans, J., 2005. Extracting a Climate Signal from 169 Glacier Records. *Science*, 308(5722): 675–677

Pettersson, R., Jansson, P., Holmlund, P., 2003. Cold Surface Layer Thinning on Storglaciären, Sweden, Observed by Repeated Ground Penetrating Radar Surveys. *Journal of Geophysical Research*: *Earth Surface*, 108(F1), doi:

10.1029/2003JF000024

Plewes, L. A., Hubbard, B., 2001. A Review of the Use of Radio-Echo Sounding in Glaciology. *Progress in Physical Geography*, 25(2): 203–236

Rippin, D., Willis, I., Arnold, N., et al., 2003. Changes in Geometry and Subglacial Drainage of Midre Lovénbreen, Svalbard, Determined from Digital Eevation Models. *Earth Surface Processes and Landforms*, 28(3): 273–298, doi:10.1002/esp.485

Rivera A, Casassa G, Bamber J, et al., 2005. Ice-Elevation Changes of Glaciar Chico, Southern Patagonia, Using ASTER DEMs, Aerial Photographs and GPS data. *Journal of Glaciology*, 51(172): 105–112

Shangguan, D. H., Liu, S. Y., Ding, Y. J., et al., 2009. Glacier Changes during the Last Forty Years in the Tarim Interior River Basin, Northwest China. *Progress in Natural Science*, 19(6): 727–732

Shangguan, D. H., Liu, S. Y., Ding, Y. J., et al., 2010. Changes in the Elevation and Extent of Two Glaciers along the Yanglonghe River, Qilian Mountains, China. *Journal of Glaciology*, 56(196): 309–317

Su, Z., Shi, Y. F., 2002. Response of Monsoonal Temperate Glaciers to Global Warming since the Little Ice Age. *Quaternary International*, 97–98: 123–131

Vincent, C., 2002. Influence of Climate Change over the 20th Century on Four French Glacier Mass Balances. *Journal of Geophysical Research*, 107(D19): 1–12, doi:10.1029/2001JD000832

Wang, P. Y., Li, Z. Q., Li, H. L., et al., 2011. Ice Surface-Elevation Change and Velocity of Qingbingtan Glacier No. 72 in the Tomor Region, Tianshan Mountains, Central Asia. *Journal of Mountain Science*, 8(6): 855–864

Wang, Y., Hou, S., Liu, Y. P., 2010. Glacier Changes in the Karlik Shan, Eastern Tien Shan, during 1971/72–2001/02. *Annals of Glaciology*, 50(53): 39–45

Welch, B. C., Pfeffer, W. T., Harper, J. T., et al., 1998. Mapping Subglacial Surfaces of Temperate Valley Glaciers by Two-Pass Migration of a Radio-Echo Sounding Survey. *Journal of Glaciology*, 44(146): 164–170

Xie, C. W., Ding, Y. J., Chen, C. P., et al., 2007. Study on the Chang of Koxkar Glacier during the Last 30 Years, Mt. Tuomuer, Western China. *Environ. Geol.*, 51(6): 1165–1170

Yao, T. D., Wang, Y. Q., Liu, S. Y., 2004. Recent Retreat of High Asian Glaciers and the Impact to Water Resource of Northwest China. *Science in China Series D*: *Earth Sciences*, 34(6): 535–543

Zhang, Y., Liu, S, Y., Shangguan, D. H., et al., 2005. Study of the Positive Degree 2 day Factors on the Koxkar Glacier on the South Slope of Tianshan Mountains. *Journal of Glaciology and Geocryology*, 27(3): 337–343 (in Chinese with English Abstract)

Zhang, Y., Fujita, K., Liu, S. Y., et al., 2010. Multi-Decadal Ice-Velocity and Elevation Changes of a Monsoonal Maritime Glacier: Hailuogou Glacier, China. *Journal of Glaciology*, 56(195): 65–74